CAMBRIDGE
UNIVERSITY PRESS

Article

Scenicite, a new uranyl-sulfate mineral from the White Canyon district, San Juan County, Utah, USA

Anthony R. Kampf[1]* , Jakub Plášil[2] , Travis A. Olds[3] , Chi Ma[4] and Joe Marty[1]

[1]Mineral Sciences Department, Natural History Museum of Los Angeles County, 900 Exposition Boulevard, Los Angeles, CA 90007, USA; [2]Institute of Physics ASCR, v.v.i., Na Slovance 1999/2, 18221 Prague 8, Czech Republic; [3]Section of Minerals and Earth Sciences, Carnegie Museum of Natural History, 4400 Forbes Avenue, Pittsburgh, Pennsylvania 15213, USA and [4]Division of Geological and Planetary Sciences, California Institute of Technology, Pasadena, California 91125, USA

Abstract

The new mineral scenicite (IMA2021-057), $[(UO_2)(H_2O)_2(SO_4)]_2 \cdot 3H_2O$, was found in the Green Lizard, Giveaway–Simplot, Markey and Scenic mines, White Canyon district, San Juan County, Utah, USA, where it occurs as a secondary phase on granular quartz matrix in association with various combinations of deliensite, gypsum, natrozippeite, rietveldite and shumwayite. Scenicite crystals are transparent, light green yellow, poorly formed blades or prisms, up to 0.1 mm in length. The mineral has white streak and vitreous lustre. It exhibits bright greenish-white fluorescence (405 nm laser). It is brittle with irregular, curved fracture and a Mohs hardness of ∼2. It has excellent {100} and good {001} cleavages. The calculated density is 3.497 g cm^{-3}. Optically, the mineral is biaxial (–) with α = 1.556(2), β = 1.573(2), γ = 1.576(2) (white light); 2V = 45(3)°; extreme $r < v$ dispersion; orientation: X = **c**, Y = **a**, Z = **b**; pleochroism: X and Y = colourless, Z = light green–yellow; and X = Y < Z. The Raman spectrum exhibits bands consistent with UO_2^{2+}, SO_4^{2-} and O–H. Electron microprobe analysis provided the empirical formula $U_{1.996}S_{2.005}O_{19}H_{13.997}$. The five strongest powder X-ray diffraction lines are [d_{obs} Å(I)(hkl)]: 7.69(70)(201), 5.63(100)(111), 4.92(84)(202,310), 4.80(93)(401) and 3.398(55)(020,120,511,601). Scenicite is orthorhombic, $Pca2_1$, a = 21.2144(15), b = 6.8188(3) c = 11.2554(6) Å, V = 1628.18(16) Å^3 and Z = 4. In the structure of scenicite (R_1 = 0.0365 for 1259 $I > 2\sigma I$), linkages of pentagonal bipyramids and tetrahedra form an infinite neutral $[(UO_2)(SO_4)(H_2O)_2]$ chain. The structure of shumwayite contains topologically identical chains.

Introduction

The mines in the Red Canyon portion of the White Canyon district in south-eastern Utah have yielded many new mineral species in recent years (e.g. Kampf *et al.*, 2021a). Most of the new species are uranyl sulfates and most, especially from the Blue Lizard mine, contain Na as an essential charge-balancing cation. The new species described herein is a uranyl sulfate, but without Na or any other cation (except H). It has been found at three of the mines in Red Canyon, but surprisingly not at the Blue Lizard mine, the world's most prolific occurrence for uranyl sulfate minerals. The mineral was found more recently in the Scenic mine, which is on Fry Mesa, ∼18 km northwest of the mines in Red Canyon. The best crystals of the new mineral were found at the Scenic mine and these made possible the full characterisation of the mineral, which has been named scenicite for this mine.

The new mineral and name (symbol Sce) were approved by the Commission on New Minerals, Nomenclature and Classification of the International Mineralogical Association (IMA2021-057, Kampf *et al.*, 2021b). The description is based on one holotype specimen from the Scenic mine and one cotype specimen from

the Green Lizard mine. Both are deposited in the collections of the Natural History Museum of Los Angeles County, 900 Exposition Boulevard, Los Angeles, CA 90007, USA, catalogue numbers 76153 (holotype) and 76154 (cotype).

Occurrence

Scenicite was first discovered on a specimen collected underground in the Green Lizard Mine (37°34′37.10″N 110°17′52.80″W) by Jerry Baird in 2015. Shortly thereafter, it was identified on specimens collected underground in the Giveaway–Simplot mine (37°33′09.80″N 110°16′58.50″W) and the Markey mine (37°32′57″N 110°18′08″W). All three of these mines are in Red Canyon, White Canyon district, San Juan County, Utah, USA. In 2020, one of the authors (JM) collected a specimen of scenicite underground in the Scenic mine (37°38′43″N 110°07′10″W) on Fry Mesa, also in the White Canyon district. The geology of all of these mines is quite similar (Chenoweth, 1993; Kampf, *et al.*, 2017a). The foregoing description of scenicite is based only on material from the Green Lizard and Scenic mines and only these should be considered cotype localities.

The uranium deposits in White Canyon district occur within the Shinarump member of the Upper Triassic Chinle Formation, in channels incised into the reddish–brown siltstones
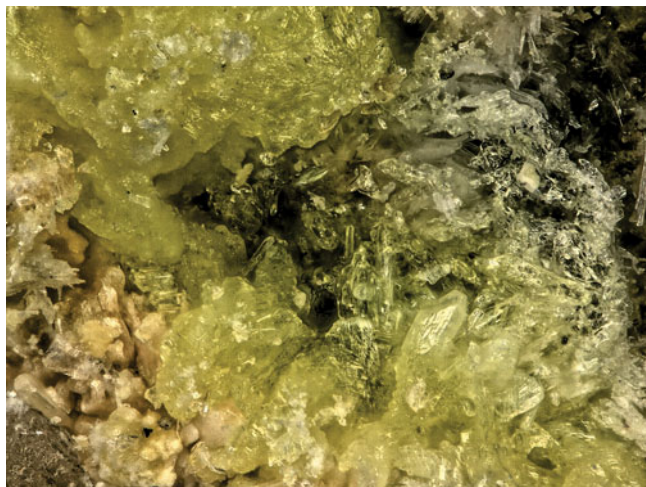
Fig. 1. Scenicite from the Scenic mine (holotype specimen #76153); field of view 0.68 mm across.

of the underlying Lower Triassic Moenkopi Formation. The Shinarump member consists of medium- to coarse-grained sandstone, conglomeratic sandstone beds and thick siltstone lenses. Ore minerals (uraninite, montroseite, coffinite, etc.) were deposited as replacements of wood and other organic material and as disseminations in the enclosing sandstone. Since the mine closed in 1982, oxidation of primary ores in the humid underground environment has produced a variety of secondary minerals, mainly carbonates and sulfates, as efflorescent crusts on the surfaces of mine walls.

Scenicite is a very rare mineral in the secondary mineral assemblages at all of its occurrences. It occurs on matrix comprised mostly of subhedral to euhedral, equant quartz crystals that are recrystallised counterparts of the original grains of the sandstone. At the Green Lizard mine, it is associated with gypsum, natrozippeite and shumwayite. At the Scenic mine, it is associated with deliensite, gypsum, rietveldite and shumwayite.

Physical and optical properties

Scenicite crystals are crude blades flattened on {100} and elongated parallel to [010]. Because crystals are generally poorly formed and occur in intergrowths, it was not possible to make morphological measurements; only the {100} form could be discerned with certainty. Crystals are up to ~0.1 mm in length and typically occur in intergrowths (Fig. 1). Crystals are light green yellow and transparent with vitreous lustre. The streak is white. The mineral fluoresces bright greenish-white under a 405 nm laser. The Mohs hardness is ~2, based upon scratch tests. Crystals are brittle with irregular, curved fracture. There is excellent cleavage on {100} and good cleavage on {001}. Scenicite is readily soluble in room-temperature H_2O. The density could not be measured because the mineral is soluble in Clerici solution. The calculated density is 3.497 g·cm^{-3} for the empirical formula and 3.506 g·cm^{-3} for the ideal formula.
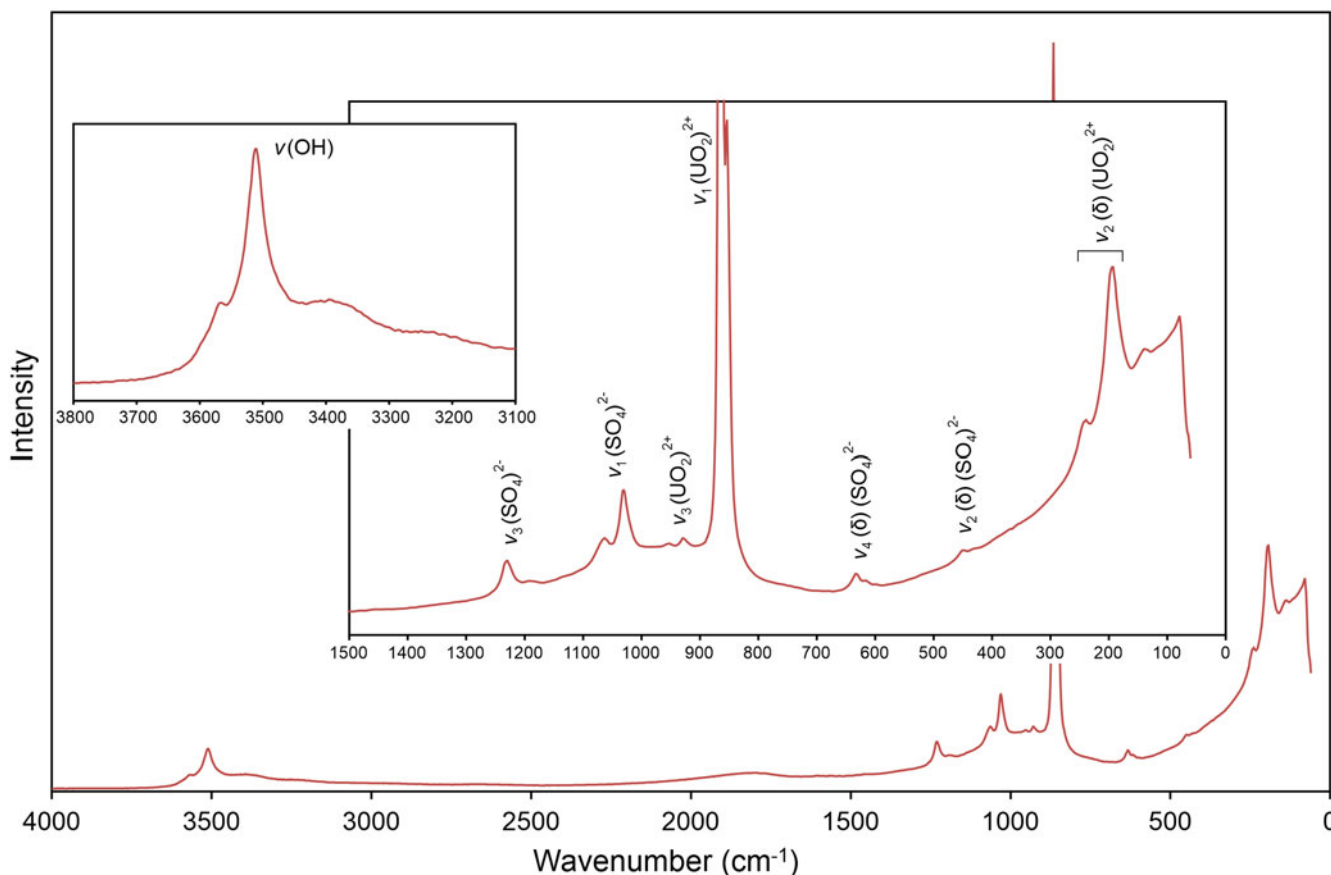

Fig. 2. Raman spectrum of scenicite recorded with a 532 nm laser.

Table 1. Chemical composition (in wt.%) for scenicite.

Constituent	Mean	Range	S.D.	Standard
UO_3	66.51	64.54–67.77	1.25	syn. UO_2
SO_3	18.70	17.92–18.99	0.43	anhydrite
H_2O*	14.69			
Total	99.90			

*Based on the structure. S.D. – standard deviation.

Optically, scenicite is biaxial (–), with $\alpha = 1.556(2)$, $\beta = 1.573(2)$ and $\gamma = 1.576(2)$ (measured in white light). The 2V measured directly on a spindle stage is 45(3)°; the calculated 2V is 45.2°. Dispersion is $r < v$, extreme. The optical orientation is $X = \mathbf{c}$, $Y = \mathbf{a}$ and $Z = \mathbf{b}$. The mineral is pleochroic with X and Y = colourless, Z = light green–yellow; and $X = Y < Z$. The Gladstone–Dale compatibility index $1 - (K_P/K_C)$ for the empirical formula is –0.005, in the superior range (Mandarino, 2007), using $k(UO_3) = 0.118$, as provided by Mandarino (1976).

Raman spectroscopy

Raman spectroscopy was conducted on a Horiba XploRA PLUS using a 532 nm diode laser, a 100 μm slit, a 1800 gr/mm diffraction grating and a 100× (0.9 NA) objective. The Raman spectrum of scenicite from 4000 to 60 cm^{-1} is shown in Fig. 2.

A broad band consisting of several overlapping vibrations in the 3650 to 3200 cm^{-1} range (the most prominent are those at 3570, 3510, 3410, 3390 and 3230 cm^{-1}) are attributed to the ν O–H stretching vibrations of the H_2O molecules. This entire suite is comparable to that observed both for shumwayite and the synthetic phase (Vlček *et al.*, 2009; Kampf *et al.*, 2017). According to the correlation given by Libowitzky (1999), the approximate O–H···O hydrogen bond-lengths range between 3.2 and 2.7 Å. In the region of the ν_2 (δ) H_2O bending vibrations, no peaks were observed, which is not unusual in Raman spectroscopy of hydrated minerals. Instead, the higher background observed there is a spectral artefact.

Table 2. Data collection and structure refinement details for scenicite.*

Crystal data	
Structural formula	$[(UO_2)(H_2O)_2(SO_4)]_2 \cdot 3H_2O$ (including unlocated H)
Crystal size (μm)	70 × 50 × 20
Space group	$Pca2_1$ (#29)
Unit cell dimensions	$a = 21.2144(15)$ Å
	$b = 6.8188(3)$ Å
	$c = 11.2554(6)$ Å
V	1628.18(16) Å^3
Z	4
Density (for above formula)	3.501 g·cm^{-3}
Absorption coefficient	20.217 mm^{-1}
Data collection	
Diffractometer	Rigaku R-Axis Rapid II
X-ray radiation/power	Mo$K\alpha$ ($\lambda = 0.71075$ Å)/50 kV, 40 mA
Temperature	293(2) K
$F(000)$	1528
θ range	3.14 to 22.44°
Reflections collected/unique	7520/1966; $R_{int} = 0.072$
Reflections with $I > 2\sigma I$	1259
Completeness to $\theta = 22.44°$	96.9%
Index ranges	$-22 \leq h \leq 22$, $-7 \leq k \leq 7$, $-12 \leq l \leq 12$
Refinement	
Refinement method	Full-matrix least-squares on F^2
Parameters/restraints	200/1
GoF	1.104
Final R indices [$I > 2\sigma I$]	$R_1 = 0.0326$, $wR_2 = 0.0753$
R indices (all data)	$R_1 = 0.0346$, $wR_2 = 0.0763$
Absolute structure parameter	0.011(12)
Largest diff. peak/hole (e^-·Å^{-3})	+2.13/–1.07

*$R_{int} = \Sigma|F_o^2 - F_o^2(\text{mean})|/\Sigma[F_o^2]$. GoF = $S = \{\Sigma[w(F_o^2 - F_c^2)^2]/(n-p)\}^{1/2}$. $R_1 = \Sigma||F_o| - |F_c||/\Sigma|F_o|$. $wR_2 = \{\Sigma[w(F_o^2 - F_c^2)^2]/\Sigma[w(F_o^2)^2]\}^{1/2}$; $w = 1/[\sigma^2(F_o^2) + (aP)^2 + bP]$ where a is 0.0285, b is 19.9 and P is $[2F_c^2 + \text{Max}(F_o^2, 0)]/3$.

Other assignments [w = weak, vw = very weak, sh = shoulder, ms = medium strong] are the band at 1230 cm^{-1} (w) with shoulder and 1180 cm^{-1} (vw), also with a shoulder, are assigned to the split triply degenerate ν_3 antisymmetric stretching vibrations of the SO_4 tetrahedra. Raman bands at 1080 (sh), 1065 (w) and 1032 (ms) cm^{-1} are assigned to the ν_1 symmetric stretching

Table 3. Atom coordinates and displacement parameters (Å^2) for scenicite.

	x/a	y/b	z/c	U_{eq}	U^{11}	U^{22}	U^{33}	U^{23}	U^{13}	U^{12}
U1	0.57989(4)	0.80710(11)	0.30017(7)	0.0187(3)	0.0255(6)	0.0142(5)	0.0164(5)	0.0015(6)	–0.0031(4)	–0.0004(4)
U2	0.70036(4)	0.29765(10)	0.68766(8)	0.0178(3)	0.0255(6)	0.0132(5)	0.0147(5)	0.0006(6)	–0.0019(5)	0.0003(3)
S1	0.6033(3)	0.3114(8)	0.4157(6)	0.0175(14)	0.026(4)	0.011(3)	0.016(3)	–0.001(3)	–0.005(3)	–0.004(2)
S2	0.6514(3)	0.8038(8)	0.5963(5)	0.0224(16)	0.035(4)	0.012(3)	0.021(4)	0.005(3)	–0.009(3)	–0.004(3)
O1	0.5484(10)	0.346(4)	0.4878(18)	0.060(7)	0.036(13)	0.102(18)	0.044(13)	0.003(13)	0.017(11)	0.005(13)
O2	0.5931(10)	0.147(3)	0.3336(16)	0.046(6)	0.072(15)	0.036(11)	0.031(13)	0.010(10)	–0.034(10)	0.005(11)
O3	0.6177(8)	0.485(2)	0.3432(13)	0.030(5)	0.045(12)	0.017(9)	0.029(11)	0.014(8)	–0.009(8)	0.008(8)
O4	0.6601(8)	0.267(2)	0.4890(14)	0.018(4)	0.027(11)	0.011(7)	0.018(9)	–0.001(7)	–0.010(7)	0.000(7)
O5	0.5893(11)	0.812(3)	0.652(2)	0.062(7)	0.067(17)	0.084(19)	0.035(13)	0.008(12)	0.012(11)	0.007(13)
O6	0.6836(10)	0.615(3)	0.6192(15)	0.042(5)	0.062(15)	0.038(12)	0.027(11)	0.007(9)	–0.023(9)	–0.012(11)
O7	0.6476(8)	0.832(2)	0.4659(14)	0.021(4)						
O8	0.6937(7)	0.965(2)	0.6440(14)	0.026(4)						
O9	0.5134(8)	0.800(2)	0.3909(17)	0.031(5)	0.015(10)	0.037(11)	0.042(12)	0.002(9)	0.003(9)	0.002(8)
O10	0.6452(8)	0.820(2)	0.2038(17)	0.033(5)	0.040(11)	0.037(10)	0.024(10)	0.010(10)	–0.018(9)	–0.002(8)
O11	0.6269(9)	0.293(2)	0.7531(15)	0.034(5)	0.045(13)	0.026(11)	0.032(11)	0.004(8)	–0.007(9)	–0.007(8)
O12	0.7757(10)	0.302(3)	0.6240(18)	0.038(5)	0.043(14)	0.038(13)	0.034(12)	–0.007(9)	0.001(9)	0.003(9)
O13	0.5222(8)	0.983(2)	0.1462(14)	0.026(4)	0.033(11)	0.016(8)	0.028(10)	0.011(8)	–0.007(7)	0.006(8)
O14	0.5263(8)	0.559(2)	0.1747(17)	0.040(5)	0.047(12)	0.030(9)	0.042(11)	0.009(11)	–0.022(10)	–0.003(8)
O15	0.7464(8)	0.515(2)	0.8336(13)	0.027(4)	0.034(10)	0.023(8)	0.024(9)	–0.011(8)	–0.014(7)	0.008(8)
O16	0.7392(9)	0.108(2)	0.8549(14)	0.037(5)	0.076(15)	0.012(9)	0.023(9)	0.011(7)	–0.029(9)	–0.008(9)
O17	0.6875(10)	0.787(3)	0.9578(18)	0.037(5)	0.046(13)	0.032(11)	0.034(12)	0.005(9)	0.006(10)	–0.001(10)
O18	0.5936(10)	0.281(3)	0.046(2)	0.054(7)	0.034(13)	0.049(14)	0.08(2)	0.005(13)	–0.008(12)	0.010(10)
O19	0.5729(15)	0.706(6)	0.893(3)	0.132(15)	0.07(2)	0.27(5)	0.053(19)	0.00(2)	–0.003(15)	–0.01(2)

Table 4. Selected bond distances (Å) for scenicite.

				Hydrogen bonds	
U1–O9	1.742(18)	U2–O11	1.72(2)	O13···O5	2.75(3)
U1–O10	1.76(2)	U2–O12	1.75(2)	O13···O18	2.78(3)
U1–O7	2.361(16)	U2–O8	2.327(16)	O14···O1	2.71(3)
U1–O2	2.36(2)	U2–O6	2.33(2)	O14···O18	2.78(3)
U1–O3	2.386(15)	U2–O4	2.403(15)	O15···O17	2.64(2)
U1–O13	2.436(15)	U2–O15	2.419(15)	O15···O3	2.89(2)
U1–O14	2.480(17)	U2–O16	2.429(15)	O16···O4	2.83(2)
<U1–O$_{ap}$>	1.751	<U2–O$_{ap}$>	1.735	O16···O17	2.70(2)
<U1–O$_{eq}$>	2.405	<U2–O$_{eq}$>	2.382	O17···O10	2.92(3)
S1–O1	1.44(2)	S2–O5	1.46(2)	O17···O19	2.60(4)
S1–O2	1.47(2)	S2–O6	1.48(2)	O18···O9	2.92(3)
S1–O3	1.472(17)	S2–O7	1.482(17)	O18···O12	2.91(3)
S1–O4	1.492(17)	S2–O8	1.517(17)	O19···O1	2.81(4)
<S1–O>	1.469	<S2–O>	1.485	O19···O5	2.83(4)

vibrations of structurally independent SO_4 tetrahedra. Some overlaps of these bands with the librations of H_2O are present (see Colmenero *et al.*, 2020).

Very weak Raman bands at 955 and 930 cm^{-1} are attributed to the v_3 antisymmetric stretching vibrations of two structurally non-equivalent uranyl ions, UO_2^{2+}. The most prominent Raman bands at 865 (vs) and 854 (s) cm^{-1} are attributed to the v_1 symmetric stretching vibration of the uranyl ions. The inferred U–O bond-lengths (after Bartlett and Cooney, 1989) of the uranyl groups, ~1.75–1.76 Å (from both v_1 and v_3), are within the range derived from the current X-ray study.

Weak bands at 632 and 618 cm^{-1} have been assigned to the v_4 (δ) triply degenerated antisymmetric stretching vibrations of SO_4 tetrahedra. Weak Raman bands 453 and 433 cm^{-1} are related to the split v_2 (δ) doubly degenerate bending vibrations of the SO_4.

A weak band at 240 cm^{-1} can be attributed by analogy (see Kampf *et al.*, 2017b; Plášil *et al.*, 2010; Colmenero *et al.*, 2020 and others) to the v_2 (δ) doubly degenerate bending vibrations of UO_2^{2+}. Nevertheless, Colmenero *et al.* (2020) showed that the

Table 5. Bond valence analysis for scenicite. Values are expressed in valence units.

	U1	U2	S1	S2	Hydrogen bonds donated	Hydrogen bonds accepted	Sum	
O1			1.63			0.22, 0.18	2.03	O
O2	0.51		1.51				2.02	O
O3	0.49		1.50			0.16	2.14	O
O4		0.47	1.43			0.17	2.07	O
O5				1.55		0.20, 0.17	1.92	O
O6		0.55		1.47			2.02	O
O7	0.51			1.46			1.98	O
O8		0.55		1.34			1.89	O
O9	1.90					0.15	2.05	O
O10	1.83					0.15	1.98	O
O11		1.99					1.99	O
O12		1.87				0.15	2.02	O
O13	0.44				−0.20, −0.19		0.04	H_2O
O14	0.40				−0.22, −0.19		−0.01	H_2O
O15		0.45			−0.26, −0.16		0.04	H_2O
O16		0.44			−0.17, −0.23		0.05	H_2O
O17					−0.15, −0.29	0.26, 0.23	0.05	H_2O
O18					−0.15, −0.15	0.19, 0.19	0.08	H_2O
O19					−0.18, −0.17	0.29	−0.07	H_2O
Sum	6.09	6.33	6.06	5.82				

Bond valence parameters from Gagné and Hawthorne (2015). Hydrogen-bond strengths are based on O–O bond lengths from Ferraris and Ivaldi (1988).
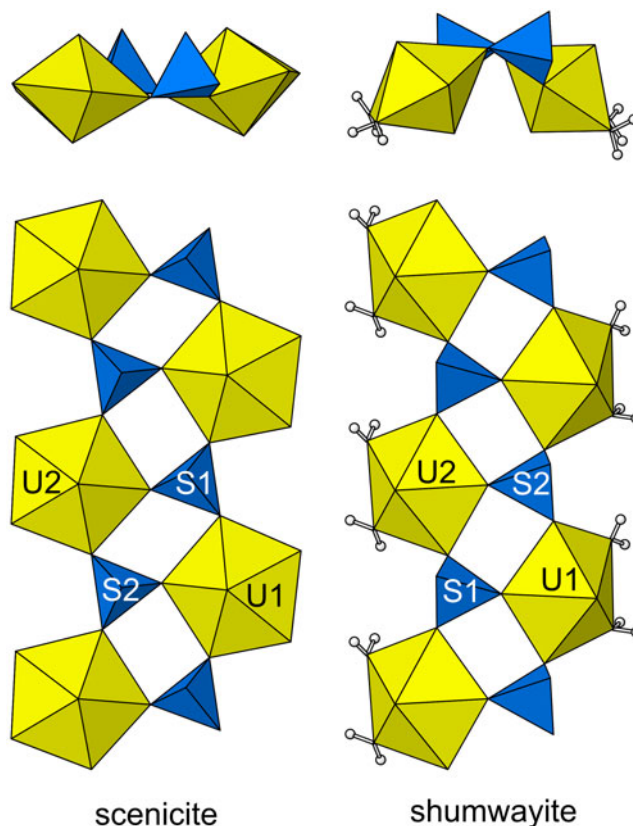
Fig. 3. The uranyl sulfate chains of formula [(UO$_2$)(SO$_4$)(H$_2$O)$_2$] along {010} in scenicite and along [100] in shumwayite. Top views are looking down the lengths of the chains. Note that the H atoms of the H$_2$O groups are shown only for shumwayite because they were not located for scenicite.

contribution of the bending energies of the uranyl ions in the structure is distributed over a wider energy region and thus, probably the strong band at 193 cm^{-1} is actually the result of energy-overlap between v_2 (δ) UO_2^{2+} and e.g. U–O$_{eq}$–(H$_2$O) stretches and bends. Weak bands at the lowest energies can be assigned to unclassified lattice modes, most probably skeletal vibrations of the entire infinite chains of polyhedra.

Chemical composition

Analyses of scenicite from the Scenic mine (6 points) were performed at Caltech on a JEOL 8200 electron microprobe in wavelength dispersive spectroscopy mode. Analytical conditions were 15 kV accelerating voltage, 10 nA beam current and 5 μm beam diameter. Insufficient material is available for CHN analysis; however, the fully ordered structure unambiguously established the quantitative content of H$_2$O. The crystals did not take a good polish, which accounts for the low analytical total. Analytical data are given in Table 1. The empirical formula (calculated on the basis of 19 O atoms per formula unit) is $U_{1.996}S_{2.005}O_{19}H_{13.997}$. The ideal formula is [(UO$_2$)(H$_2$O)$_2$(SO$_4$)]$_2$·3H$_2$O, which requires UO$_3$ 66.65, SO$_3$ 18.66, H$_2$O 14.69, total 100 wt.%.

X-ray crystallography and structure refinement

Powder X-ray diffraction was done using a Rigaku R-Axis Rapid II curved imaging plate microdiffractometer, with monochromatised
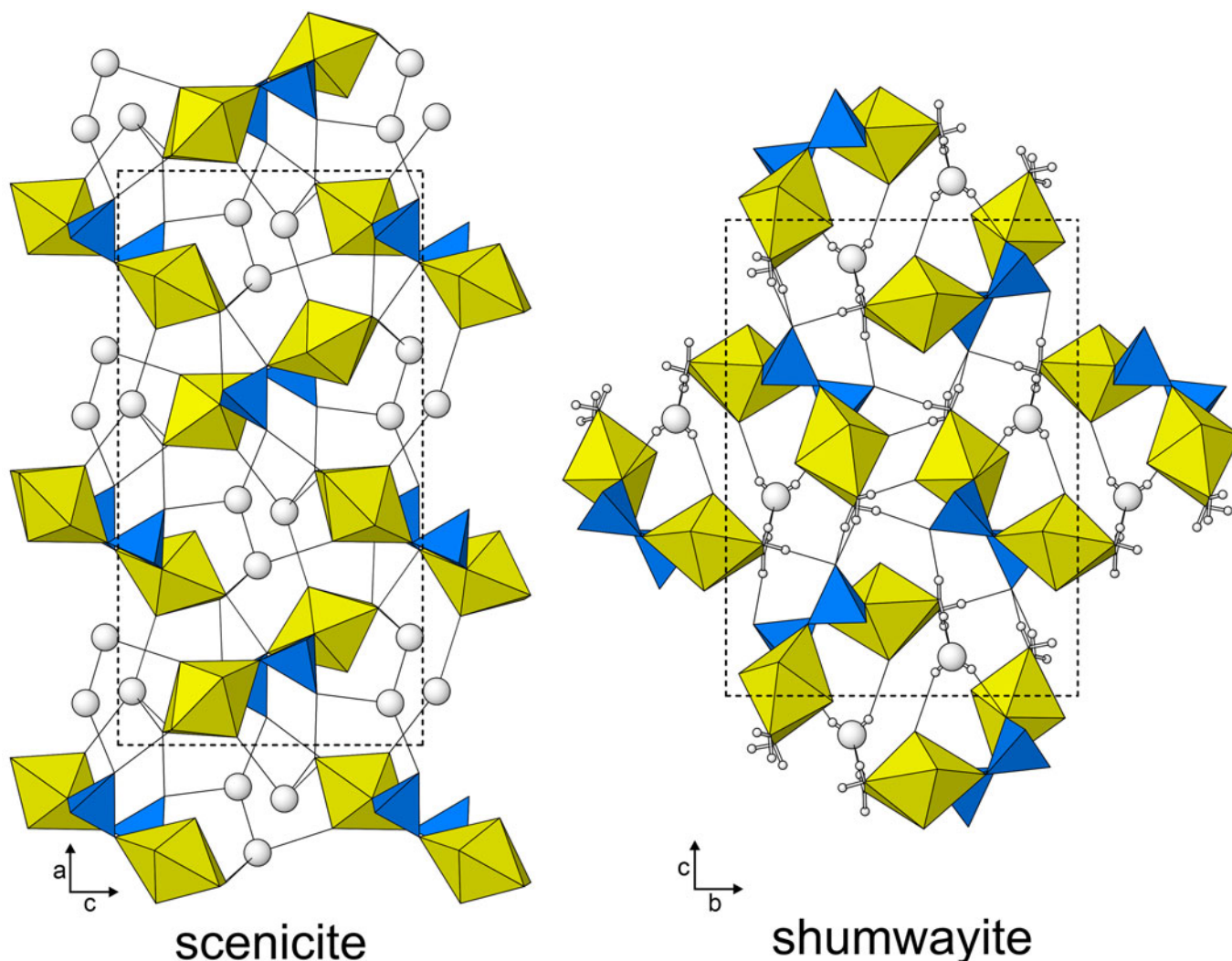
Fig. 4. The structures of scenicite (viewed down [010]) and shumwayite (viewed down [100]). The O atoms of the isolated H_2O groups are shown as large white balls. The H atoms of the H_2O groups (small white balls) are shown only for shumwayite. The hydrogen bonds are shown with thin black lines. The unit-cell outlines are shown with dashed lines.

Mo$K\alpha$ radiation. A Gandolfi-like motion on the φ and ω axes was used to randomise the sample and observed *d* values and intensities were derived by profile fitting using *JADE Pro* software (Materials Data, Inc.). The powder data are presented in Supplementary Table S1.

The single-crystal structure data were collected at room temperature using the same diffractometer and radiation noted above. Data were collected for crystals from both the Green Lizard and Scenic mines. The resulting structures were essentially identical. The refinement using the Scenic mine data was superior, so only it is reported here.

The Rigaku *CrystalClear* software package was used for processing structure data, including the application of an empirical multi-scan absorption correction using *ABSCOR* (Higashi, 2001). The structure was solved using the intrinsic-phasing algorithm of the *SHELXT* program (Sheldrick, 2015a) and was found to be the same as that of the synthetic phase reported by Zalkin *et al.* (1978). Refinement proceeded by full-matrix least-squares on F^2 using *SHELXL-2016* (Sheldrick, 2015b). All non-hydrogen atom sites were refined successfully with anisotropic displacement parameters except for O7 and O8, which had to be refined

isotropically. Difference-Fourier synthesis failed to locate H atom positions. Data collection and refinement details are given in Table 2, atom coordinates and displacement parameters in Table 3, selected bond distances in Table 4, and a bond valence analysis in Table 5. The crystallographic information file has been deposited with the Principal Editor of *Mineralogical Magazine* and is available as Supplementary material (see below).

Description and discussion of the structure

The two U sites (U1 and U2) in the structure of scenicite are surrounded by seven O atoms forming a squat UO$_7$ pentagonal bipyramid. This is the most typical coordination for U^{6+}, particularly in uranyl sulfates, where the two short apical bonds of the bipyramid constitute the uranyl group. Three of the five equatorial O sites of the UO$_7$ bipyramid participate in two different SO$_4$ tetrahedra (centred by S1 and S2); the other two equatorial O sites are H_2O groups. The linkages of pentagonal bipyramids and tetrahedra form an infinite neutral $[(UO_2)(SO_4)(H_2O)_2]$ chain along [010] (Fig. 3). There are three isolated H_2O groups located

between the chains. The chains and isolated H_2O groups are linked together by hydrogen bonds (Fig. 4).

The structure of shumwayite, $[(UO_2)(SO_4)(H_2O)_2]_2 \cdot H_2O$ (Kampf *et al.*, 2017b), contains topologically identical chains; however, the chains in the two structures are rather different geometrically (Fig. 3). Both structures contain isolated H_2O groups between the chains, and the chains and isolated H_2O groups are linked together by hydrogen bonds (Fig. 4); however, there is only one isolated H_2O group between the chains in the shumwayite structure. Burns (2005) lists eight uranyl sulfates, chromates and selenates, including the synthetic equivalents of scenicite and shumwayite, with topologically identical chains. It is also worth noting that scenicite and shumwayite occur in intimate association at both cotype localities.

Uranyl sulfate minerals that contain no charge-balancing cations other than H are rare; they number just five out of the currently 57 known species: besides scenicite, these include jáchymovite, $(UO_2)_8(SO_4)(OH)_{14} \cdot 13H_2O$ (Čejka *et al.*, 1996), shumwayite (Kampf *et al.*, 2017b), uranopilite, $(UO_2)_6(SO_4)O_2(OH)_6 \cdot 14H_2O$ (Burns, 2001) and metauranopilite, $(UO_2)_6(SO_4)(OH)_{10} \cdot 5H_2O$ (Frondel, 1952). More than 20 synthetic phases are known in the same 'cation-less' $U–SO_4–H_2O/OH$ system, including the heptahydrated synthetic analogue of scenicite. Interestingly, the heptahydrate is dimorphous, crystallising as the α form (the analogue of scenicite) and the metastable monoclinic β form. The preparation of both phases is straightforward. Zalkin *et al.* (1978) crystallised the α form from an aqueous solution of uranyl sulfate and (+)-tartaric acid, which they allowed to evaporate slowly. Leroy *et al.* (1965) prepared the β form by mixing stoichiometric amounts of UO_3 and sulfuric acid, which they heated and left to crystallise in air. After several days, crystals of a tetrahydrate, $UO_2SO_4(H_2O)_4$, were formed, after which the remaining, less-concentrated mother liquor was left to crystallise slowly again in air and crystals of the β form of the pentahydrate crystallised.

These syntheses may provide some insight into how scenicite formed. Previously, we have noted that very small differences in pH, $U:SO_4$ and H_2O content generates a wide variety of crystal-chemically unique uranyl sulfate phases, and such could be the case here; however, differences in stability of the dimorphs may contribute to the formation of scenicite. Cordfunke (1972) reports that the synthetic analogue of shumwayite, $UO_2SO_4 \cdot 2.5H_2O$, forms from the β phase in a moist environment. Although different synthesis routes for the α form probably exist, it may suggest that organic acid templation is an important step in the crystallisation of scenicite. The paragenetic relationship between scenicite and shumwayite is not clear from the samples we have studied, but like most uranyl minerals in the region, both have crystallised in close proximity to asphaltite and we have noted that other organically templated uranyl minerals (the oxalates uroxite and metauroxite) occur at several localities.

References

Bartlett J.R. and Cooney R.P. (1989) On the determination of uranium-oxygen bond lengths in dioxouranium(VI) compounds by Raman spectroscopy. *Journal of Molecular Structure*, **193**, 295–300.

Burns P.C. (2001) A new uranyl sulfate chain in the structure of uranopilite. *The Canadian Mineralogist*, **39**, 1139–1146.

Burns P.C. (2005) U^{6+} minerals and inorganic compounds: insights into an expanded structural hierarchy of crystal structures. *The Canadian Mineralogist*, **43**, 1839–1894.

Čejka J., Sejkora J., Mrazek Z., Urbanec Z. and Jarchovsky T. (1996) Jáchymovite, $(UO_2)_8(SO_4)(OH)_{14} \cdot 13H_2O$, A new uranyl mineral from Jáchymov, the Krusne Hory Mts., Czech Republic, and its comparison with uranopilite. *Neues Jahrbuch für Mineralogie – Abhandlungen*, **170**, 155–170.

Chenoweth W.L. (1993) The Geology and Production History of the Uranium Deposits in the White Canyon Mining District, San Juan County, Utah. *Utah Geological Survey Miscellaneous Publication*, 93–3.

Colmenero F., Plášil J. and Němec I. (2020) Uranosphaerite: Crystal structure, hydrogen bonding, mechanics, infrared and Raman spectroscopy and thermodynamics. *Journal of Physics and Chemistry of Solids*, **141**, 109400.

Cordfunke E.H.P. (1972) The system uranyl sulphate-water—ii: Phase relationships and thermochemical properties of the phases in the system $UO_3–SO_3–H_2O$. *Journal of Inorganic and Nuclear Chemistry*, **34**, 1551–1561.

Ferraris G. and Ivaldi G. (1988) Bond valence vs bond length in $O \cdots O$ hydrogen bonds. *Acta Crystallographica Section B*, **44**, 341–344.

Frondel C. (1952) Studies of uranium minerals (X): Uranopilite. *American Mineralogist*, **37**, 950–959.

Gagné O.C. and Hawthorne F.C (2015) Comprehensive derivation of bond-valence parameters for ion pairs involving oxygen. *Acta Crystallographica*, B71, 562–578.

Higashi T. (2001) *ABSCOR. Rigaku Corporation*, Tokyo.

Kampf A.R., Plášil J., Kasatkin A.V., Marty J. and Čejka J. (2017a) Klaprothite, péligotite and ottohahnite, three new sodium uranyl sulfate minerals with bidentate $UO_7–SO_4$ linkages from the Blue Lizard mine, San Juan County, Utah, USA. *Mineralogical Magazine*, **80**, 753–779.

Kampf A.R., Plášil J., Kasatkin A.V., Marty J. Čejka J. and Lapčák L. (2017b) Shumwayite, $[(UO_2)(SO_4)(H_2O)_2]_2 \cdot H_2O$, a new uranyl sulfate mineral from Red Canyon, San Juan County, Utah, USA. *Mineralogical Magazine*, **81**, 273–285.

Kampf A.R., Olds T.A., Plášil J., Nash B.P. and Marty J. (2021a) Uranoclite, a new uranyl-chloride mineral from the Blue Lizard mine, San Juan County, Utah, USA. *Mineralogical Magazine*, **85**, 438–443.

Kampf A.R., Plášíl J., Olds T.A., Ma C. and Marty J. (2021b) Scenicite, IMA 2021-057. CNMNC Newsletter 63. *Mineralogical Magazine*, 85, 910–915, https://doi.org/10.1180/mgm.2021.74

Leroy J.-M., Tudo J. and Tridot G. (1965) Sur les hydrates du sulfate d'uranyle. *Comptes Rendus Hebdomadaires des Séances de L'Académie Des Sciences*, **260**, 5802–5805.

Libowitzky E. (1999) Correlation of O–H stretching frequencies and O–H···O hydrogen bond lengths in minerals. *Monatshefte für Chemie*, **130**, 1047–1059.

Mandarino J.A. (1976) The Gladstone-Dale relationship – Part 1: derivation of new constants. *The Canadian Mineralogist*, **14**, 498–502.

Mandarino J.A. (2007) The Gladstone–Dale compatibility of minerals and its use in selecting mineral species for further study. *The Canadian Mineralogist*, **45**, 1307–1324.

Plášil J., Buixaderas E., Čejka J., Sejkora J., Jehlička J. and Novák M. (2010) Raman spectroscopic study of the uranyl sulphate mineral zippeite: low wavenumber and U–O stretching regions. *Analytical and Bioanalytical Chemistry*, **397**, 2703–2715.

Sheldrick G.M. and IUCr (2015a) *SHELXT* – Integrated space-group and crystal-structure determination. *Acta Crystallographica*, A71, 3–8.

Sheldrick G.M. and IUCr (2015b) Crystal structure refinement with *SHELXL*. *Acta Crystallographica*, C71, 3–8.

Vlček V., Čejka J., Císařová I., Goliáš V. and Plášil J. (2009) Crystal structure of $UO_2SO_4 \cdot 2.5H_2O$: Full anisotropic refinement and vibration characterization. *Journal of Molecular Structure*, **936**, 75–79.

Zalkin A., Ruben H. and Templeton D.H. (1978). Structure of a new uranyl sulfate hydrate. A-$2UO_2SO_4 \cdot 7H2O$. *Inorganic Chemistry*, **17**, 3701–3702.